Applied Surface Science 257 (2011) 4031–4037

Contents lists available at ScienceDirect

Applied Surface Science

journal homepage: www.elsevier.com/locate/apsusc

Structural and optical properties of ZnO thin films prepared by sol–gel method with different thickness

Linhua Xu[a,*], Xiangyin Li[b], Yulin Chen[a], Fei Xu[a]

[a] Physics Experiment Center, Nanjing University of Information Science & Technology, Nanjing 210044, China
[b] Department of Applied Physics, Nanjing University of Science and Technology, Nanjing 210094, China

ARTICLE INFO

Article history:
Received 31 August 2010
Received in revised form
23 November 2010
Accepted 25 November 2010
Available online 3 December 2010

PACS:
61.05.cp
68.37.Ps
68.55.−a
78.55.Et

Keywords:
ZnO thin films
Film thickness
Sol–gel method
Growth mode
Optical properties

ABSTRACT

In this work, ZnO thin films with different thickness were prepared by sol–gel method on glass substrates and the structural and optical properties of these films were studied by X-ray diffractometer, atomic force microscope, UV–visible spectrophotometer, ellipsometer and fluorophotometer, respectively. The structural analyses show that all the samples have a wurtzite structure and are preferentially oriented along the *c*-axis perpendicular to the substrate surface. The growth process of highly *c*-axis oriented ZnO thin films derived from sol–gel method is a self-template process. With the increase of film thickness, the structural disorder decreases and the crystalline quality of the films is gradually improved. A transition of crystal growth mode from vertical growth to lateral growth is observed and the transition point is found between 270 and 360 nm thickness. The optical analyses show that with the increase of film thickness, both the refractive index and ultraviolet emission intensity are improved. However, the transmittance in the visible range is hardly influenced by the film thickness, and the averages are all above 80%.

1. Introduction

As a new-generation multifunctional semiconductor material, ZnO thin film has received extensive attention in recent years. Due to the direct wide band-gap of 3.37 eV and a large exciton binding energy of 60 meV at room temperature, ZnO thin films are considered as the ideal materials for the fabrication of short-wavelength optoelectronic devices such as ultraviolet lasers [1], ultraviolet light-emitting diodes [2], ultraviolet photoconductive detectors [3]. ZnO thin films usually have high transmittance in the visible range and possess excellent n-type conductivity when doped with Al, Ga and In, so they can be used as transparent electrodes [4] and window layers [5] in solar cells. Furthermore, ZnO thin films also have potential applications in thin film transistors [6], optical waveguides [7], gas sensors [8], diluted magnetic semiconductor devices [9], and surface acoustic wave devices [10] and so on.

So far, ZnO thin films have been prepared by many techniques such as molecular beam epitaxy, atomic layer epitaxy, metal-organic chemical vapor deposition, spray pyrolysis, sol–gel method, pulsed laser deposition, magnetron sputtering, electron beam evaporation. Among these techniques, sol–gel method attracts much attention due to some distinct advantages including low cost, simple deposition equipment, easier adjustment of composition, being able to carry out doping at molecular level, easy fabrication of large-area films and so on. Many research groups have prepared ZnO thin films by sol–gel method and used them to fabricate opto-electronic devices. For example, Ma et al. used the sol–gel derived ZnO thin films to fabricate ultraviolet random laser [1]; Park et al. utilized the sol–gel derived ZnO thin films to fabricate thin film transistor [11]; Kyaw et al. applied the sol–gel derived ZnO thin films to organic solar cell [12]. Although the sol–gel method is a relatively simple technique for preparing ZnO thin films, there are still many factors affecting the physical properties of ZnO thin films. These factors include ZnO sol concentration [13], preheating temperature [14], post-annealing temperature [15], annealing atmosphere [16], film thickness [17] and so on. Among these factors, the influence of film thickness on structural, optical and electrical properties of ZnO thin films (especially undoped ZnO thin films) derived from sol–gel method was less studied. Even for the previously reported results, there are still many differences between them. For example, Sharma and Mehra [17] prepared

* Corresponding author.
E-mail addresses: congyu3256@tom.com, congyu3256@sina.com (L. Xu).

0169-4332/$ – see front matter © 2010 Elsevier B.V. All rights reserved.
doi:10.1016/j.apsusc.2010.11.170

highly *c*-axis oriented ZnO thin films by sol–gel method; they found a transition of growth mode from vertical growth to lateral growth of the ZnO thin film with the increase of thickness. Mridha and Basak [18] also prepared ZnO thin films with different thicknesses by sol–gel method. However, these films were basically randomly oriented except that one with 260 nm thickness which was preferentially oriented along the *c*-axis direction. No transition of growth mode was observed, but Mridha et al. found that the ZnO thin film with 260 nm thickness had the best crystallization, optical and electrical properties. In order to obtain high-quality optoelectronic devices based on ZnO thin films, it is very important to deeply investigate the influence of the film parameters such as film thickness on the microstructure and optical properties. In this work, ZnO thin films with different thickness were prepared by the optimized sol–gel technique on glass substrates and the structural and optical properties were deeply studied. Based on the analyses of X-ray diffraction (XRD) and atomic force microscope (AFM), a growth mechanism of highly *c*-axis oriented ZnO thin films derived from sol–gel method was proposed.

2. Experiments

The ZnO sol was prepared using zinc acetate, anhydrous ethanol and monoethanolamine (MEA) as the solute, solvent and sol stabilizer, respectively. Zinc acetate was first dissolved in ethanol, and then the resulting solution was stirred by a magnetic stirring apparatus in hot water bath at 70 °C. At the same time, MEA was put into the solution drop by drop. The molar ratio of MEA to zinc acetate was kept at 1.0. After 2 h, a transparent ZnO sol was formed. In the sol, the Zn concentration was 0.35 mol/L. After the ZnO sol was aged for 24 h at room temperature, ZnO thin films were prepared by dip-coating this ZnO sol on glass substrates which had been thoroughly cleaned and dried. After each coating, the sample was first placed under an infrared lamp to be dried for 8 min, and then was put into a furnace at 350 °C for preheating treatment for 6 min. The above-mentioned procedures from dip-coating to a preheating treatment were repeated for 3, 6, 9 and 12 times in order to get the films with different thicknesses; correspondingly, the films were labeled as samples A, B, C and D, respectively. All the samples were post-annealed at 500 °C in air for 1 h. The average thickness of each single layer measured by an ellipsometer was ~30 nm. Therefore, the thickness of samples A, B, C and D was about 90, 180, 270 and 360 nm, respectively.

The crystal phase and crystalline orientation of the ZnO thin films were analyzed by an X-ray diffractometer with a Bragg–Brentano geometry (Bruker D8 Advance). The surface morphology was observed by an atomic force microscope (CSPM4000) in contact mode. The film thickness and refractive index were measured by an ellipsometer (TPY-2). The transmittance was recorded by a UV–visible spectrophotometer (TU-1901). The photoluminescence spectra were used to study the luminescent property of the films. The light source was a Xe lamp and the excitation wavelength was 325 nm. All the measurements were performed in air at room temperature.

3. Results and discussion

3.1. The dependence of structural property of ZnO thin film on thickness

Fig. 1 shows XRD patterns of ZnO thin films with different thickness. All the diffraction peaks in the patterns correspond to the reflection of wurtzite-structured ZnO planes and all the samples have a strong (0 0 2) peak. This suggests that all the prepared ZnO thin films have a hexagonal wurtzite structure and are preferentially oriented along the *c*-axis perpendicular to the substrate surface. As for sample A, besides the (0 0 2) peak, it still has two other peaks, namely (1 0 0) peak and (1 0 1) peak. With the increase of film thickness, the intensity of (0 0 2) peak is increased, but the full width at half maximum (FWHM) is decreased as shown in Fig. 2. The similar results were also reported by others [19,20]. It means that within a certain range of thickness, the crystalline quality of ZnO thin films is gradually improved with the increase of film thickness. The positions of the (0 0 2) peaks are shown in Fig. 2. The strain along the *c*-axis for the samples was calculated by the following formula:

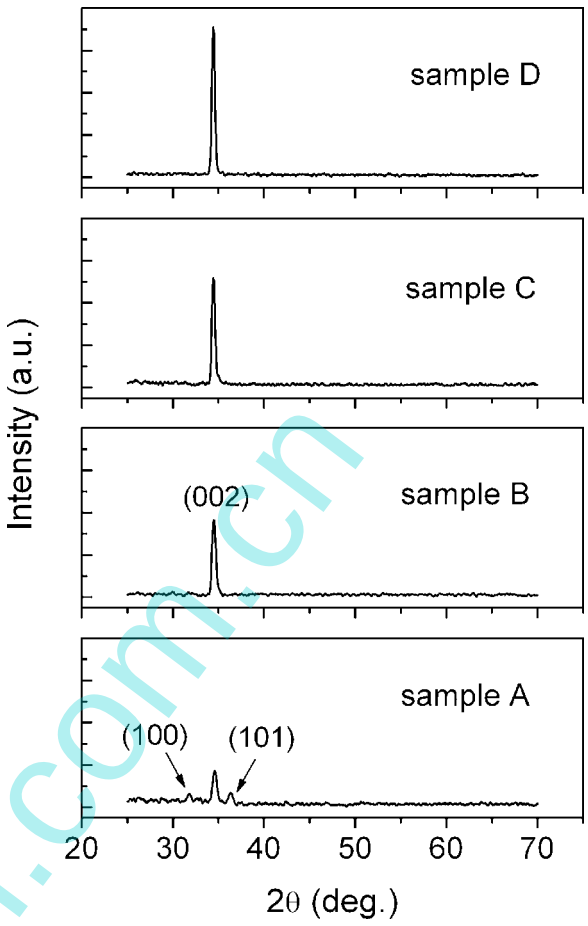

Fig. 1. XRD patterns of ZnO thin films with different thickness.

$$\varepsilon = \frac{c - c_0}{c_0} \times 100\% \quad (1)$$

where c is the lattice parameter of the sample calculated from XRD data and c_0 is lattice parameter of ZnO crystal without strain. From Fig. 2, it can be seen that the strain gradually decreases with the increase of film thickness. This is similar to the result reported by Dong et al. [19]. However, Mridha and Basak [18] found that the strain along the *c*-axis is decreased as the film is grown up to a thickness of 300 nm. Above 300 nm, the strain again becomes appreciable. We think the difference of strain in ZnO thin films prepared by us and Mridha et al. is mainly connected with the preparation conditions and thermal treatment. For example, in the film preparation process, we adopted three-step thermal treatment, namely infrared drying, pre-heating at 350 °C, and post-annealing at 500 °Cfor 1 h, but Mridha and Basak [18] adopted two-step thermal treatment, namely drying at 120 °C and annealing at 550 °C for 30 min. In fact, a 30-min annealing time is not long enough to eliminate the strain in the film. Therefore, from

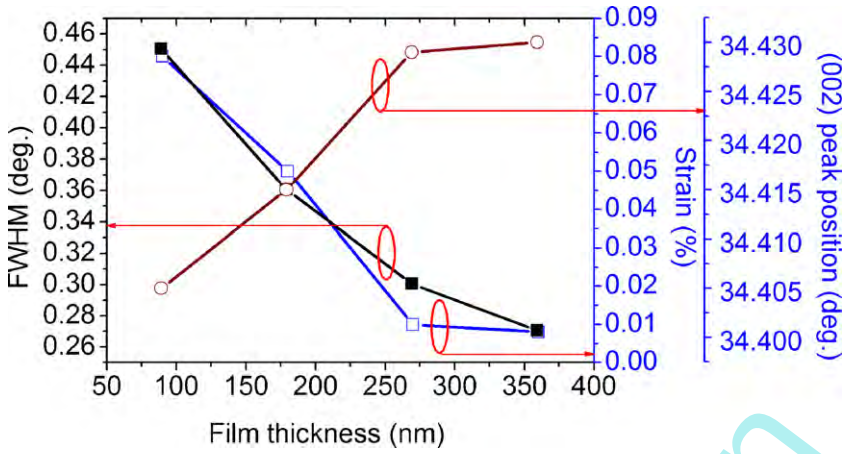

Fig. 2. The FWHM, position of (0 0 2) peak and the strain along the *c*-axis for ZnO thin films with different thickness.

the above results, it is evident that a good thermal treatment can largely decrease the film strain and improve its crystallization. It should be noted that the infrared drying is important for reducing the strain and improving the film quality. The results about the effect of infrared drying on ZnO thin films will be reported later elsewhere.

Fig. 3 shows the two-dimensional (left) and three dimensional (right) surface morphology images of the samples. It is obvious that the surfaces of these films are very smooth. The RMS roughness is 4.04, 3.68, 3.70 and 3.56 nm for samples A, B, C and D, respectively. Form the three-dimensional surface morphology images, it can be seen that ZnO thin films comprise columnar grains which grow along the *c*-axis direction perpendicular to the substrate surface. This is in agreement with the results of XRD. From the two-dimensional surface morphology images, it can be seen that when the film thickness is less than 270 nm, the in-plane grain size does not change much and only a small part of the grains increased with the increasing film thickness. The grain boundaries are clear and the grains are round shape in plane. It means that the growth mode of ZnO grains is mainly vertical growth [19]. However, when the film thickness reaches 360 nm, the in-plane grain size is obviously increased and grain boundaries are not clear yet. This suggests that the growth mode varied with the increase of film thickness. That is to say, when the film thickness is less than 270 nm, the growth mode of ZnO grains is mainly vertical growth; when the film thickness reaches 360 nm, the growth mode has been translated from vertical to lateral growth. The transition point is found between 270 and 360 nm thickness. The lateral growth made ZnO film much denser. When Sharma and Mehra [17] studied the physical properties of Al and Co co-doped ZnO thin films prepared by sol–gel method, they found a transition of ZnO grains from vertical to lateral growth with the increase of film thickness and the transition point was found between 250 and 360 nm thickness. Moreover, when Dong et al. [19] studied the physical properties of Al-doped ZnO thin films deposited by pulsed laser deposition, they also found a transition of growth mode from vertical growth to lateral growth with the increasing film thickness; the transition point was found between 70 and 120 nm thickness. From the above results, it can be known that although a transition of growth mode from vertical growth to lateral growth is found in all the above-mentioned three studies, the transition point is different from one another. Comparing our result with that of Sharma and Mehra [17], it can be seen that the possible range of the transition point is lapped each other to a large extent. This is mainly because both of us adopted the sol–gel method to prepare ZnO thin films and used the similar thermal treatments. However, ZnO thin films prepared by Sharma et al. are co-doped with Al and Co. The incorporation of Al and Co maybe affected the normal growth of ZnO crystals; correspondingly, the transition point of growth mode is somewhat different from that of undoped ZnO thin films. Obviously, the range of transition point determined by Dong et al. [19] is very different from those observed by us and Sharma et al. It probably resulted from the two factors, namely the different deposition techniques for ZnO thin films and the different annealing treatments. The growth mode transition is considered due to the decrease of strain in the grains with the increase of film thickness.

3.2. The growth mechanism of highly c-axis oriented ZnO thin films derived from sol–gel method

So far, many research groups have prepared highly *c*-axis oriented ZnO thin films by sol–gel method [16,17]. That ZnO thin films are preferentially oriented along the *c*-axis is connected with the nature of ZnO as well as film preparation conditions. Owing to the minimum surface free energy of the (0 0 2) plane [21], the (0 0 2) direction (namely, *c*-axis orientation) of a ZnO thin film is the most thermodynamically favorable growth direction. This is the intrinsic factor leading to ZnO crystals preferentially growing along the *c*-axis orientation. For example, Ohyama et al. [22] and Dong et al. [19] prepared highly *c*-axis oriented ZnO thin films on glass substrates by sol–gel method and pulsed laser deposition, respectively. Since the glass is an amorphous material, there is no epitaxial relationship between ZnO and the substrate. However, these ZnO thin films are not randomly oriented. Furthermore, Dong et al. [19] found that even if the ZnO thin film is as thin as 15 nm, it is still oriented along the *c*-axis. These results indicate that the intrinsic factor plays a very important role for ZnO crystals to be preferentially oriented along the *c*-axis. On the other hand, the film preparation conditions are the extrinsic factors affecting the growth orientation of ZnO thin films. For example, for the ZnO thin films deposited by sol–gel method, the sol stabilizer has an important effect on crystal orientation. Some research results [22,23] indicate that MEA as the sol stabilizer is favorable for the formation of highly *c*-axis oriented ZnO thin films, but DEA and TEA as the sol stabilizer are unfavorable for the formation of highly *c*-axis oriented ZnO thin films.

Several growth mechanisms of highly *c*-axis oriented ZnO thin films deposited by sol–gel method have been proposed up to now. For example, Wang et al. [23] think that the growth of highly *c*-axis oriented ZnO thin films is a self-assembly process in which a dipole–dipole interaction between the polar nanograins plays a great role for the crystal growth. A sketch of the ZnO thin film self-assembly mechanism along the *c*-axis was given in Ref. [23].

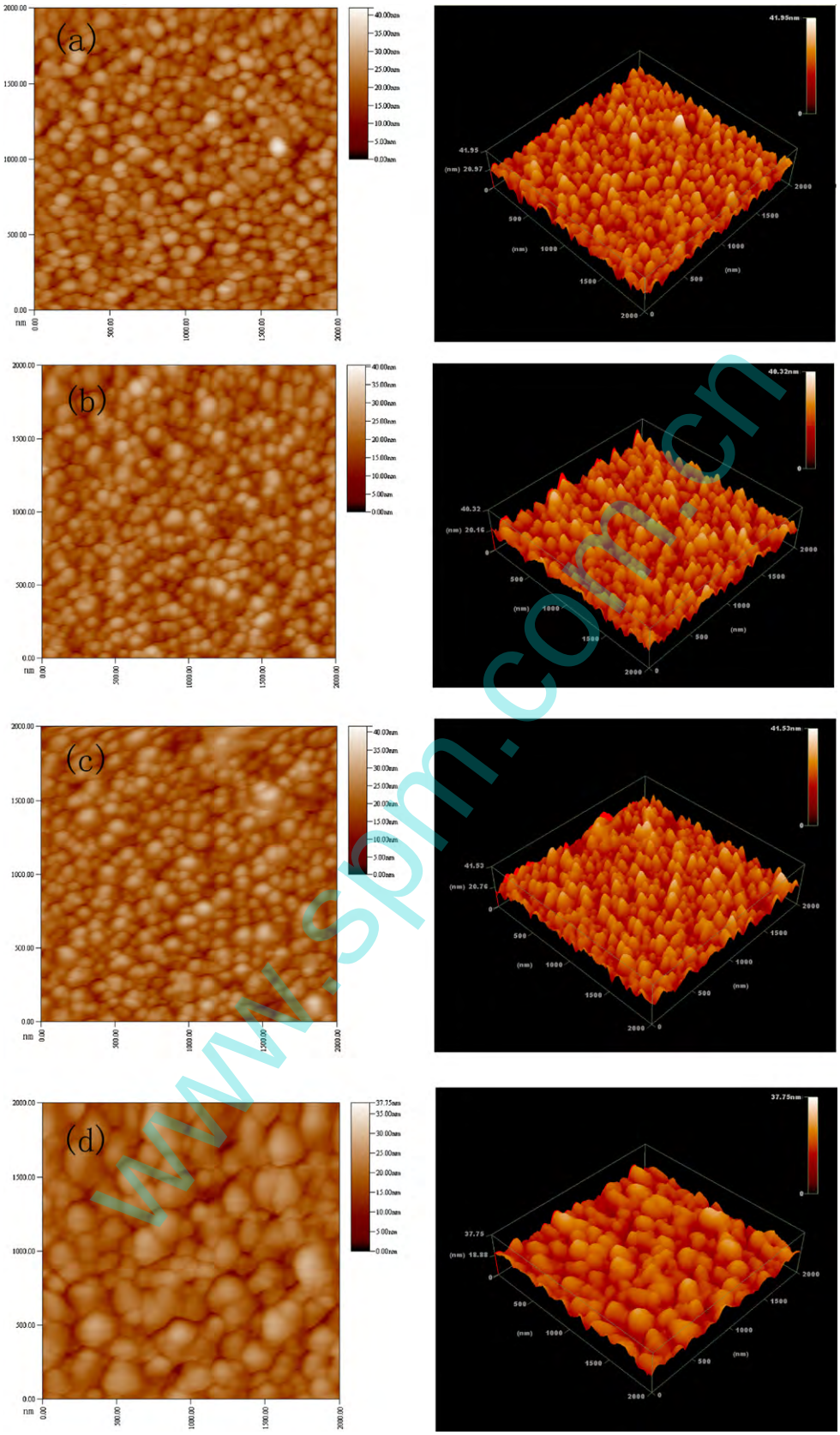

Fig. 3. Two-dimensional (left) and three-dimensional (right) surface morphology images of sample A (a), B (b), C (c) and D (d).

For another example, Zhu et al. [24] propose that the growth of highly *c*-axis oriented ZnO thin film is a self-buffer layer process in which every layer will act as a buffer layer for next one, promoting a heterogeneous nucleation process.

The authors think that the growth process of highly *c*-axis oriented ZnO thin films deposited by sol–gel method is not only a self-assembly process but also a self-template process. A schematic sketch of the growth mechanism of self-template process is shown

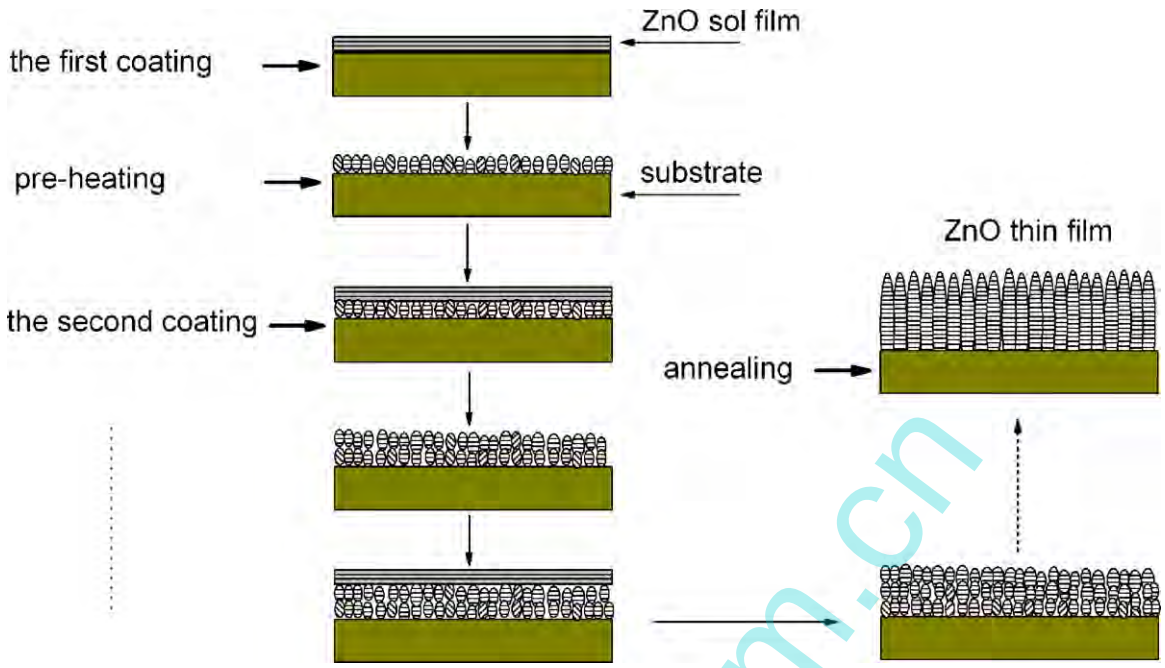

Fig. 4. The schematic sketch of the growth mechanism of self-template process.

in Fig. 4. After the first layer of ZnO sol film was coated and preheated, the nuclei were formed and gradually grew into crystals. Since the glass substrate is an amorphous material, the nuclei should be randomly oriented; correspondingly, the crystals were also randomly oriented. However, the (0 0 2) plane of ZnO has the minimum surface free energy [21], so most of the crystals grew preferentially along the (0 0 2) direction (namely, the *c*-axis direction) and only a small part of crystals grew along other directions. After the second layer of ZnO sol film was coated and preheated, the new crystals were formed using the former layer as a growth template; therefore, some new crystals still grew along other directions rather than the (0 0 2) direction. This can explain why sample A has the (1 0 0) and (1 0 1) peaks besides the (0 0 2) peak. However, with the increase of the film thickness, the grains begin to coalesce and grow in a direction to minimize the energy of substrate-film interface and free surface energy [17]. In the single-layer crystal growth process, the interaction between ZnO crystals played a dominant role for the growth orientation. Because the crystals along the (0 0 2) direction grow faster, those crystals growing along other directions are soon suppressed [25]. When the third layer crystals were formed, they were nearly all oriented along the (0 0 2) direction. After the total layers were coated, the ZnO thin film was post-annealed. In the annealing process, the diffusion and migration of atoms between neighboring layers happened. Finally, columnar grains through the entire film thickness were formed. The ZnO thin film deposited by sol–gel method is a multi-layered system. However, when the film was given a suitable annealing treatment including appropriate annealing temperature and time, the resulting ZnO thin film has no interface between neighboring layers and in fact formed an entire single layer, which has been observed in many studies [24]. It should be pointed out that a suitable annealing treatment is very important for the formation of ZnO thin films with columnar structure by sol–gel method. For example, Zhu et al. [24] found that the columnar structure can be formed only after a certain incubation time from a film that featured a granular grain structure.

The sol–gel technique is a wet-chemical method. The film deposition process by the sol–gel method is very different from those by other techniques such as pulsed laser deposition, magnetron sputtering, electron beam evaporation. Accordingly, the total growth process of ZnO thin films including nucleation, crystal growth, coarsening is also very different for the sol–gel method and other physical deposition methods. The studies on the growth mechanisms of ZnO thin films prepared by sol–gel method is very important for getting high-quality films applied to optoelectronic devices.

3.3. The dependence of optical properties of ZnO thin films on thickness

Fig. 5 presents the optical transmittance spectra of ZnO thin films with different thickness. It is clear that all the samples have high transmittance in the visible range and the average is about 83%. Therefore, within the range from 90 to 360 nm, film thickness has almost no effect on the transmittance. However, compared with samples A, B, and C, sample D has more uniform transmittance in the whole visible range (400–700 nm). This may be due to the decreased optical scattering caused by the decrease of grain boundary density owing to the increase of grain size. From the above

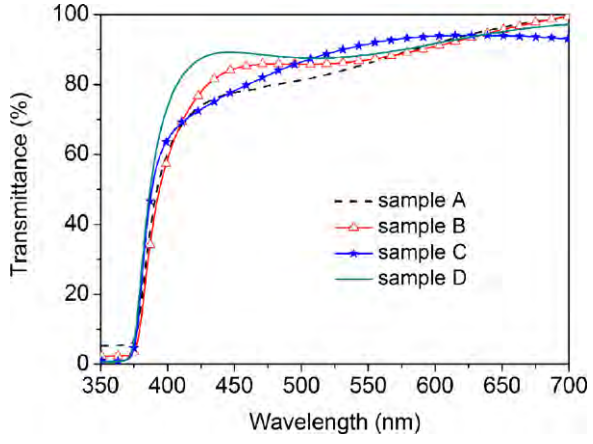

Fig. 5. Transmittance spectra of ZnO thin films with different thickness.

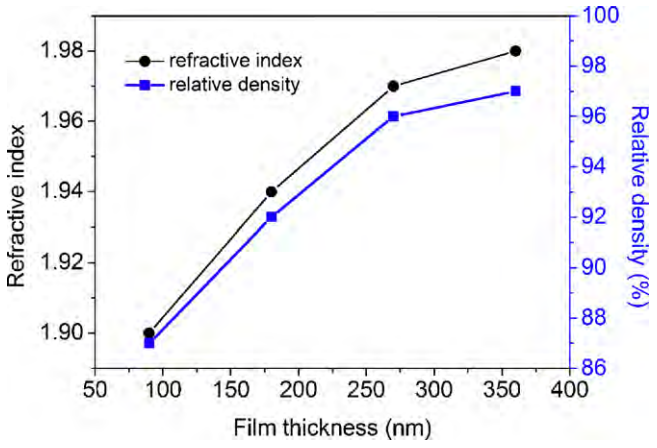

Fig. 6. The refractive indexes and relative density of the samples.

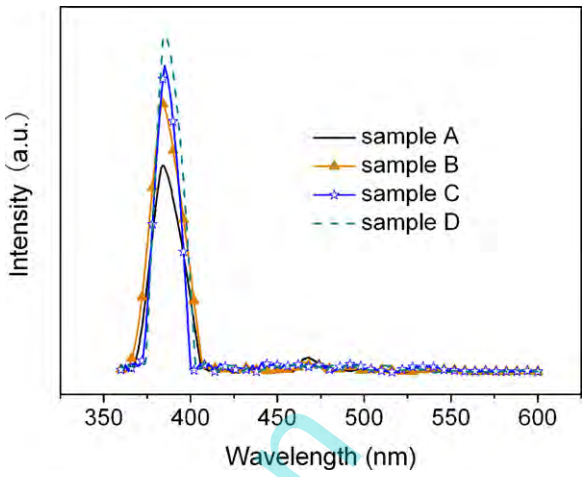

Fig. 7. Room-temperature photoluminescence spectra of the samples.

results, it can be known that ZnO thin films prepared by sol–gel method have high transmittance in the visible range, which can be used as transparent window materials in many optoelectronic devices [26]. Furthermore, it should be mentioned that Sharma and Mehra [17] found that the transmittance of Co and Al co-doped ZnO thin films prepared by sol–gel method decreased in the visible range when the film thickness was more than 200 nm. They thought that the increase of scattering owing to the large roughness in thicker films and oxygen vacancies resulted in decrease in optical transmittance.

Fig. 6 shows the variation of refractive index (at $\lambda = 632.8$ nm) and the relative density as a function of film thickness. Refractive index is an important parameter reflecting the optical quality of ZnO thin films. At the same time, it can also reflect the crystallinity of ZnO thin films. Fig. 6 gives the refractive indexes of the samples measured by an ellipsometer. When the samples were measured, three measurement points were randomly selected on each sample. The average of the three measured values was used as the refractive index of the sample. The relative density is also a parameter which can reflect the degree of crystallization of ZnO thin films. The relative density can be calculated using the formula [22]:

$$d = \frac{n^2 - 1}{n_0^2 - 1} \times 100\% \quad (2)$$

where n is the refractive index of the sample and n_0 is the refractive index of single crystal ZnO ($n_0 = 2.0$). From Fig. 6, it can be seen that both the refractive index and the relative density are improved with the increase of film thickness, indicating the crystalline quality of ZnO thin films is gradually improved [27]. Furthermore, it should be pointed out that the refractive index and relative density become more uniform on the whole film when the film thickness is more than 270 nm. The authors think the variation of the refractive index and the relative density is mainly connected with the growth mode transition of grains. The growth mode transition from vertical growth to lateral growth improved the uniformity of ZnO thin film. With the increase of film thickness, the film becomes denser and denser. Accordingly, the refractive index and relative density become more uniform.

Fig. 7 shows the room-temperature photoluminescence spectra of the ZnO thin films with different thickness. All the samples have a strong ultraviolet emission peak centered at 383 nm. It is generally ascribed this ultraviolet emission to the recombination of free excitons. Many research groups have reported the sol–gel derived ZnO thin films with good ultraviolet emission performance [16,28,29]. Taschuk et al. [29] found that the ZnO thin films prepared by sol–gel method have higher ultraviolet emission efficiency than those prepared by pulsed laser deposition, sputtering and electron beam evaporation. This is probably connected with the unintentional incorporation of hydrogen [30] in the ZnO thin films prepared by sol–gel method. It can be seen from Fig. 7 that with the increase of film thickness, the ultraviolet emission gradually gets stronger. However, when the film thickness is above 180 nm, the increased magnitude of ultraviolet emission is decreased. The ultraviolet emission efficiency of ZnO thin films is mainly dependent on the crystalline quality. The higher the crystallization is, the higher the density of free excitons is, and correspondingly the stronger the ultraviolet emission is. Therefore, the increased ultraviolet emission is attributed to the improvement of the crystalline quality with the increase of film thickness. Also, it can be noticed from Fig. 7 that besides the ultraviolet emission peak, sample A still has a very weak blue emission peak centered at 465 nm which is possibly associated with Zn interstitial defects [31]. When the ZnO film is relatively thin, its structural disorder is relatively large and some interstitial Zn atoms exist, which possibly lead to the blue emission. With the increase of film thickness, the structural disorder decreases [32] and the density of Zn interstitial defect is reduced. As a result, the blue emission is also decreased.

4. Conclusion

In this work, ZnO thin films with various thicknesses were prepared by sol–gel method and the structural and optical properties were deeply investigated. The structural analysis showed that all the ZnO thin films were highly *c*-axis oriented. With the increase of film thickness, the crystalline quality of ZnO thin film was improved and the growth mode of grains gradually turned from vertical growth to lateral growth. In the range from 90 to 360 nm, the film thickness had almost no effect on the transmittance in the visible range, but the refractive index and ultraviolet emission were improved with the increase of film thickness. The growth mode transition was found to have effect on the physical properties of ZnO thin films: on the one hand, it makes the film much denser; on the other hand, it makes the optical properties more uniform on the whole film. The authors speculate that the preparation conditions like ZnO sol concentration, doping, etc. and the thermal treatments have an influence on the growth mode transition. It needs more investigation to uncover the relationship between them. These studies will be beneficial to more deeply understand the growth behavior of ZnO thin films derived from sol–gel method.

References

[1] X. Ma, P. Chen, D. Li, Y. Zhang, D. Yang, Appl. Phys. Lett. 91 (2007) 251109.
[2] W.S. Han, Y.Y. Kim, B.H. Kong, H.K. Cho, Thin Solid Films 517 (2009) 5106.

[3] K.W. Liu, J.G. Ma, J.Y. Zhang, Y.M. Lu, D.Y. Jiang, B.H. Li, D.X. Zhao, Z.Z. Zhang, B. Yao, D.Z. Shen, Solid State Electron. 51 (2007) 757.
[4] B.Y. Oh, M.C. Jeong, T.H. Moon, W. Lee, J.M. Myoung, J.Y. Hwang, D.S. Seo, J. Appl. Phys. 99 (2006) 124505.
[5] Y. Hagiwara, T. Nakada, A. Kunioka, Sol. Energy Mater. Sol. Cells 67 (2001) 267.
[6] D.H. Levy, D. Freeman, S.F. Nelson, P.J. Cowdery-Corvan, L.M. Irving, Appl. Phys. Lett. 92 (2008) 192101.
[7] C.L. Jia, K.M. Wang, X.L. Wang, X.J. Zhang, F. Lu, Opt. Exp. 13 (2005) 5093.
[8] S.S. Badadhe, I.S. Mulla, Sens. Actuators B 143 (2009) 164.
[9] X.C. Liu, E.W. Shi, Z.Z. Chen, H.W. Zhang, L.X. Song, H. Wang, S.D. Yao, J. Cryst. Growth 296 (2006) 135.
[10] S. Krishnamoorthy, A.A. Iliadis, Solid State Electron. 52 (2008) 1710.
[11] W.J. Park, H.S. Shin, B.D. Ahn, G.H. Kim, S.M. Lee, K.H. Kim, H.J. Kim, Appl. Phys. Lett. 93 (2008) 083508.
[12] A.K.K. Kyaw, X.W. Sun, C.Y. Jiang, G.Q. Lo, D.W. Zhao, D.L. Kwong, Appl. Phys. Lett. 93 (2008) 221107.
[13] M. Dutta, S. Mridha, D. Basak, Appl. Surf. Sci. 254 (2008) 2743.
[14] Y.S. Kim, W.P. Tai, S.J. Shu, Thin Solid Films 491 (2005) 153.
[15] M. Wang, E.J. Kim, J.S. Chung, E.W. Shin, S.H. Hahn, K.E. Lee, C. Park, Phys. Status Solidi (a) 203 (2006) 2418.
[16] P.T. Hsieh, Y.C. Chen, M.S. Lee, K.S. Kao, M.C. Kao, M.P. Houng, J. Sol–Gel Sci. Technol. 47 (2008) 1.
[17] M. Sharma, R.M. Mehra, Appl. Surf. Sci. 255 (2008) 2527.
[18] S. Mridha, D. Basak, Mater. Res. Bull. 42 (2007) 875.
[19] B.Z. Dong, G.J. Fang, J.F. Wang, W.J. Guan, X.Z. Zhao, J. Appl. Phys. 101 (2007) 033713.
[20] J.H. Lee, J. Electroceram. 23 (2009) 512.
[21] N. Fujimura, T. Nishihara, S. Goto, J. Xu, T. Ito, J. Cryst. Growth 130 (1993) 269.
[22] M. Ohyama, H. Kozuka, T. Yoko, Thin Solid Films 306 (1997) 78.
[23] J. Wang, Y. Qi, Z. Zhi, J. Guo, M. Li, Y. Zhang, Smart Mater. Struct. 16 (2007) 2673.
[24] M.W. Zhu, J.H. Xia, R.J. Hong, H. Abu-Samra, H. Huang, T. Staedler, J. Gong, C. Sun, X. Jiang, J. Cryst. Growth 310 (2008) 816.
[25] S. Nicolay, S. Fay, C. Ballif, Cryst. Growth Des. 9 (2009) 4957.
[26] J.C. Lee, K.H. Kang, S.K. Kim, K.H. Yoon, I.J. Park, J. Song, Sol. Energy Mater. Sol. Cells 64 (2000) 185.
[27] F.K. Shan, G.X. Liu, W.J. Lee, G.H. Lee, I.S. Kim, B.C. Shin, Y.C. Kim, J. Cryst. Growth 277 (2005) 284.
[28] S.K. Mohanta, S.H. Lee, B.H. Kong, H.K. Cho, J. Cryst. Growth 311 (2009) 1539.
[29] M.T. Taschuk, J.M. Laforge, H. Nguyen, Y.W. Sun, P. Kursa, R.G. DeCorby, M.J. Brett, Y.Y. Tsui, Phys. Status Solidi (c) 6 (2009) s31.
[30] A. Dev, R. Niepelt, J.P. Richters, C. Ronning, T. Voss, Nanotechnology 21 (2010) 065709.
[31] X.Q. Wei, Z.G. Zhang, M. Liu, C.S. Chen, G. Sun, C.S. Xue, H.Z. Zhuang, B.Y. Man, Mater. Chem. Phys. 101 (2007) 285.
[32] L. Miao, S. Tanemura, M. Tanemura, S.P. Lau, B.K. Tay, J. Mater. Sci.: Mater. Electron. 18 (2007) s343.